

## Article

# Hosting Capacity Estimate Based on Photovoltaic Distributed Generation Deployment: A Case Study in a Campus of the University of São Paulo

Igor Cordeiro <sup>1,2,\*</sup> , Welson Bassi <sup>1,2</sup>  and Ildo Luís Sauer <sup>1,2</sup> 

<sup>1</sup> Institute of Energy and Environment (IEE), University of São Paulo (USP), São Paulo 05508-010, Brazil; welson@iee.usp.br (W.B.); illsauer@iee.usp.br (I.L.S.)

<sup>2</sup> Center for Analysis, Planning and Energy Resources Development (CPLEN), São Paulo 05508-010, Brazil

\* Correspondence: igor.cordeiro@alumni.usp.br

**Abstract:** Distributed generation, which is mainly deployed with PV systems that benefit economically prosumers, has soared in use in Brazil. Despite this, PV capacity in excess may cause technical issues which concern planning engineers who have adopted rules of thumb to screen interconnection requests without any detailed study. Recently, the hosting capacity concept has been employed to assess how much PV capacity a distribution grid can host without deteriorating grid parameters, reliability, or power quality. A steady-state and worst-case-based scenario was used to run deterministic power flow simulations to estimate the hosting capacity of a specific radial circuit at a campus of the University of São Paulo, referred to as “USP-105”. Although the result may be not completely accurate, it was found that USP-105 can accommodate 103% of its peak load or 4970.6 kW of PV power, which reduced the circuit’s annual peak load by 9%. Another finding was that hosting capacity increased when PV-DG deployment was dispersed along the circuit rather than concentrated on a single location (e.g., closest, or furthest to the substation). Utilities may therefore benefit from a simple and quick assessment to obtain an overview of how specific circuits behave on PV deployment and indicate which locations are technically more beneficial.

**Keywords:** photovoltaic; distributed generation; hosting capacity; power flow; utility



**Citation:** Cordeiro, I.; Bassi, W.; Sauer, I.L. Hosting Capacity Estimate Based on Photovoltaic Distributed Generation Deployment: A Case Study in a Campus of the University of São Paulo. *Energies* **2023**, *16*, 3934. <https://doi.org/10.3390/en16093934>

Academic Editors: Zhengmao Li, Tianyang Zhao, Ke Peng, Jinyu Wang, Zao Tang and Sumedha Sharma

Received: 18 April 2023

Revised: 2 May 2023

Accepted: 4 May 2023

Published: 6 May 2023



**Copyright:** © 2023 by the authors. Licensee MDPI, Basel, Switzerland. This article is an open access article distributed under the terms and conditions of the Creative Commons Attribution (CC BY) license (<https://creativecommons.org/licenses/by/4.0/>).

## 1. Introduction

In recent years, solar photovoltaic (PV) module prices have plummeted, bringing down total costs per installed capacity [1] and consequently making solar PV electricity very competitive compared with traditional energy resources in utility-scale projects; therefore, PV capacity reached about 710 GW worldwide by the end of 2020 [2]. Due to the affordability of the technology—even for very low-capacity installations—and local regulation, distributed generation (DG) has expanded intensely, especially with the deployment of residential rooftop PV systems which are interconnected to the distribution grid. In Brazil, since the Brazilian Electricity Regulatory Agency (ANEEL) regulated DG nationwide in 2012, PV-DG has reached 17.2 GW as of December 2022 [3]; three-quarters of PV systems are residential installations, and almost a third of the total installed capacity comprises commercial-size systems.

Most countries have adopted net energy metering (NEM) as an energy compensation scheme, thus PV-DG system capacity is commonly oversized to meet daily energy demand. While owners of such systems—also called prosumers—are benefiting from reduced bills, distribution utilities may have technical issues if PV-DG capacity is in excess. When PV power is not consumed instantaneously by the local load, it is then injected into the grid and may cause technical problems, of which voltage variation is one of the most significant issues [4]. This leads the grid to operate in conditions that are abnormal to those for which it was originally designed, i.e., under the paradigm that power flows unidirectionally from

substations to passive consumer loads [5]. Power injection in excess may cause voltage rise at low load situations [6], leading to overvoltage and fast voltage variation. This is particularly the case when high penetration of PV-DG is concentrated near the end of long and lightly loaded feeders [7], but voltage impacts tend to be the least severe when concentrated near the substation [8]. On the other hand, properly located PV-DG can reduce feeder losses [9] and mitigate voltage drops along distribution feeders [6].

Reverse power flow might still cause thermal overloading of cables and transformers, frequency variation, harmonic distortions, and premature failure of equipment, as well as malfunctioning of protection devices. All these issues are of great concern considering the fact that PV-DG power generation is uncontrollable and has a variable nature due to weather conditions. Moreover, utilities do not know in advance where and how much capacity will be installed, nor they can reject interconnection requests that comply with the requirements, so unrestricted growth of PV-DG capacity may lead to undesirable consequences to reliability and power quality. The imminence of those serious issues would require reinforcement and upgrades to allow more capacity to be interconnected. However, if it is known how much capacity a feeder can accommodate without changes, there will be no adverse impacts and thus no reinforcement or upgrades are needed. On the contrary, utilities could benefit from that and even postpone infrastructure investments. The amount of PV-DG a feeder can host is known as hosting capacity (HC).

### *1.1. Concept and Assessment of Hosting Capacity*

The term HC was first introduced in the context of DG by André Even in 2004, who presented a methodology to determine HC as a general approach for renewable energy integration in distribution grids [10]; the term was refined by Bollen and Hassan in 2011 [9] and theoretical applications were included. The authors defined HC as the amount of new production or consumption that can be connected to the grid without endangering the reliability or voltage quality of other customers [11]. The maximum capacity of PV-DG or any other distributed energy resource (DER) a feeder can host without causing adverse impacts [12] or requiring infrastructure upgrades [13] outline the same concept but in other words.

A common rule of thumb used in the U.S. permitted interconnection requests without a detailed impact study if the PV-DG capacity was up to 15% of the feeder's peak load, saving time and reducing costs to the utilities [8]. This was a fast-screening approach many distribution-planning engineers used based on the observation that typical residential distribution feeders have minimum daily loads of approximately 30% of their annual peak loads [13]. The 15% rule of thumb is conservative to prevent any operating grid parameter from being violated. Ismael et al. (2019) discussed other international experiences and practical rules of thumb for DG interconnection that also served as a preliminary HC estimate. However, as the aggregate PV-DG capacity increases, additional impact studies should be performed and become more important over time.

### *1.2. Performance Indices and Limits*

To begin any HC study, it is essential to know which grid parameters—also referred to as performance indices—and their respective acceptable limits will be considered in the assessment [10]. That said, HC is not when the performance begins to deteriorate, but when the deterioration becomes unacceptable [14]. Shayani and Oliveira (2011) presented a theoretical framework to determine the maximum amount of PV-DG in radial distribution systems considering two basic steady-state grid parameters as performance indices: voltage rise and conductor ampacity [15]. In many other real case studies examined by Ismael et al. (2019), both overvoltage and thermal overloading were the common performance indices considered. Crucially, HC depends on both PV-DG capacity and location and voltage impacts tend to be worst issue when PV-DG is concentrated at the feeder end [16]; thus, HC is lower in the sections of a radial feeder far from the substation and higher when PV-DG is closest to a substation [13].

Besides this, the availability of data and a suitable method play a key role in determining the HC. Mulenga et al. (2020) presented a literature review on methods and compared deterministic, stochastic, and time series methods that can be used to determine the HC. Each method has its advantages and drawbacks and choosing one of them is a trade-off between which accuracy is needed, what data is available (from the grid, load, and PV-DG), how much time can be dedicated to method implementation, and what is the computational effort for resolution.

Deterministic methods are straightforward; they use known data that do not change in simulation runs, so no uncertainty is taken into consideration. The amount of PV-DG is the only variable that is incremented each time the power flow analysis—which is used as a tool—checks if the limits of the performance indices have not been reached yet. Although deterministic methods are easier to implement and quick to resolve, impact and HC tend to be overestimated and underestimated, respectively. Stochastic methods simulate aleatory uncertainties such as PV power and demand, and epistemic uncertainties such as PV system capacity and its location [10]. Often, probabilistic approaches with Monte Carlo simulations are used. Although results provided by stochastic methods are probabilistically more realistic, simulations can run for hours.

This paper is a case study of a real radial circuit referred to as “USP-105” in the campus Cidade Universitária “Armando de Salles Oliveira” (CUASO, São Paulo, Brazil) of the University of São Paulo (USP, São Paulo, Brazil), located in the city of São Paulo, Brazil. For this study, voltage rise and current-carrying capacity (ampacity) of conductors were selected as performance indices, and a static and worst-case-based scenario approach was considered. An algorithm was implemented to run deterministic power flow analysis and perform HC estimation based on certain conditions. In addition to that, three different simulations returned HC values concerning (i) circuit load, (ii) a well-accepted conception that HC is higher when PV-DG is closer to the substation, and finally (iii) what the HC is if PV-DG is concentrated or dispersed along the USP-105 main feeder. Therefore, the main question this paper intends to answer is how much PV-DG capacity USP-105 can host, considering the methods and conditions selected, compared to the circuit’s peak load. Thus, this paper aims to demonstrate that the applied method provides a rational, technically based alternative to the usual conservative rule of thumb approaches. Therefore, utilities can use it as a better method to actively admit and locate PV-DG for their own and other consumers’ benefit.

## 2. Case Study: USP-105 Feeder

The CUASO grid is constituted of five circuits directly buried underground. USP-105 is a 13.8 kV radial circuit whose main feeder extends 3.3 km from the campus substation (ETD-USP) through the west and south side of the campus. The cross-sectional area of the main feeder is  $3 \times 240 \text{ mm}^2$  and laterals are  $3 \times 70 \text{ mm}^2$  or  $3 \times 35 \text{ mm}^2$  (represented by the red, blue, and green lines on Figure 1, respectively). Twelve CUASO educational and research centers (load centers) are served by USP-105: Institute of Energy and Environment (IEE, São Paulo, Brazil), PUSP-C (Prefecture of the USP Campus, São Paulo, Brazil), NUCEL (Cellular and Molecular Therapy Center, São Paulo, Brazil), HU (University Hospital, São Paulo, Brazil), FOFITO (Department of Physiotherapy, Speech Therapy and Occupational Therapy, São Paulo, Brazil), ICB (Institute of Biomedical Sciences, São Paulo, Brazil), FO (School of Dentistry, São Paulo, Brazil), FMVZ (School of Veterinary Medicine and Animal Science, São Paulo, Brazil) and IB (Institute of Biosciences, São Paulo, Brazil). Figure 1 shows a map of CUASO and the USP-105 main feeder and its laterals.

The USP-105 circuit can be represented by a 23-bus diagram numbered from 0 (substation ETD-USP) to 22. Some buses are tap-off nodes (buses 1, 3, 5, 7, 9, 10, 13, 15, 18, and 21) and the others are load buses: IEE (bus 2), PUSP-C (bus 4), NUCEL (bus 6), HU (bus 8), ICB III (bus 11), FOFITO (bus 12), FO (bus 14), ICB IV (bus 16), FMVZ (bus 17), ICB II (bus 19), ICB I (bus 20) and IB (bus 22). Figure 2 shows the USP-105 single-line diagram.



Figure 1. USP-105 feeder along CUASO.

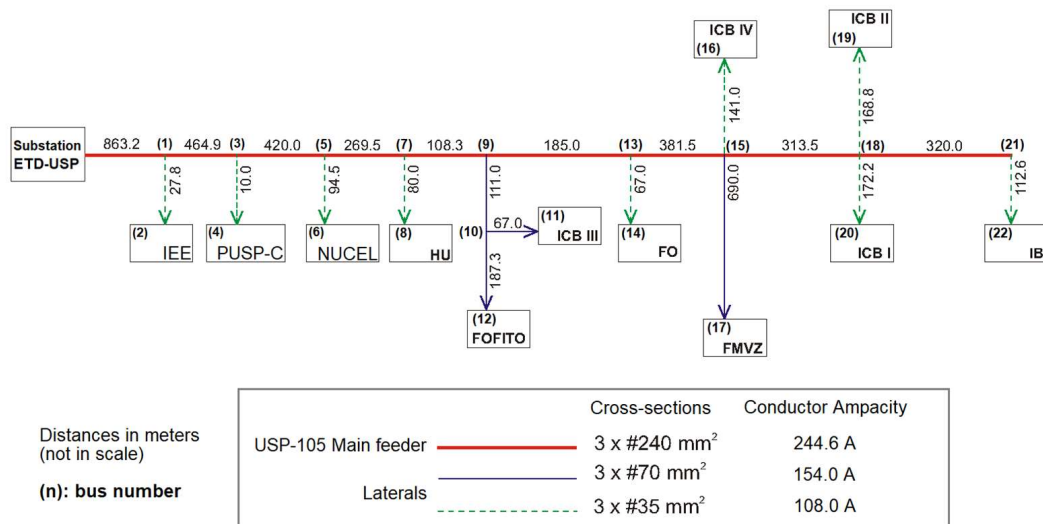
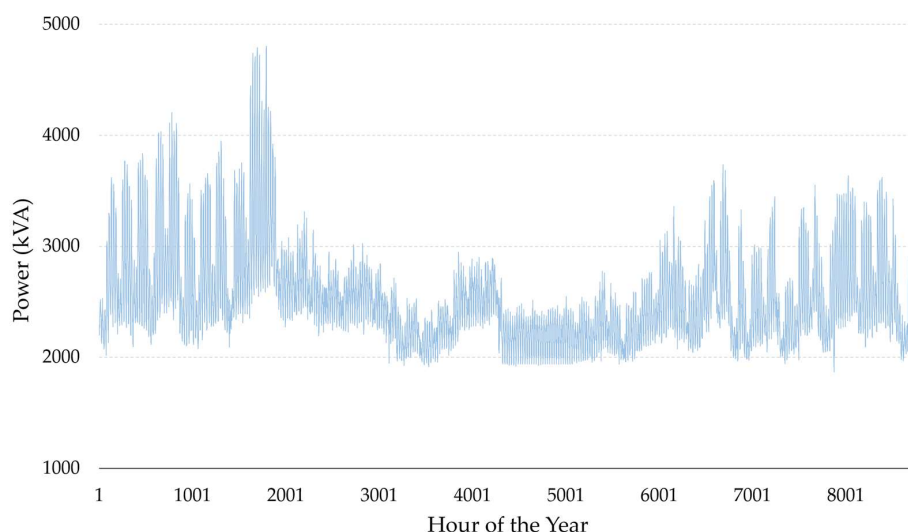


Figure 2. USP-105 feeder single-line diagram.

### 2.1. USP-105 Load

A supervisory system implemented at CUASO, based on a Supervisory Control and Data Acquisition (SCADA) platform, performs minute-by-minute measurements of power (active, reactive, and apparent), power factor, voltage, and current in the campus. The active and reactive power values of the twelve load centers served by the USP-105 were used in this case study, however, average values were considered at 1-h intervals (from hour 1 to 8760) for a whole year, considering data acquired up to March 2021. Figure 3 shows the aggregate USP-105 load power.



**Figure 3.** Aggregate USP-105 load power.

The circuit’s peak load (4804.6 kVA) occurred on 16 March at 3 p.m. (hour 1791 of the year) and the minimum load (1867.5 kVA) occurred on 25 November at 3 a.m. (hour 7875). According to the data, the highest load power values were concentrated in the afternoon, mainly between 2 p.m. and 5 p.m.

2.2. Existing PV-DG at CUASO

CUASO already has 624 kW of PV-DG, composed of various PV arrangements, of which two are interconnected to USP-105 at IEE: (i) a 156.0 kW ground installation and (ii) a 78.0 kW rooftop installation at an IEE office building. A third 84.5 kW rooftop system is installed at HU. The PV power in kW refers, unless otherwise specified, to the rated power of the solar modules, i.e., the direct current (DC) power.

2.3. PV-DG Power Modelling at CUASO

The existing PV-DG data was not available, so a synthetic 8760-h data series was created to model the PV power generation for the existing as well as the simulated PV systems. All PV systems simulated were assumed to have fixed arrays whose tilt angle is 24°, approximately equal to the local latitude (23°36’ south) and faced north (azimuth angle is 0°).

The irradiation data was acquired from the website of the Reference Center of Solar and Wind Energy Sérgio Brito (CRESESB) which is part of Electric Power Research Center (CEPEL) [17] and receives financial support from the Brazilian Ministry of Mines and Energy. Table 1 shows the daily average irradiation incident on the plane of the PV arrays.

**Table 1.** Daily average irradiation for each month.

Month	Jan	Feb	Mar	Apr	May	Jun	Jul	Aug	Sep	Oct	Nov	Dec
R [kWh·m <sup>-2</sup> ·day <sup>-1</sup> ]	4.72	5.20	4.81	4.68	4.23	4.10	4.14	4.98	4.46	4.58	4.73	5.04

The method used to determine the output power generated by a PV system consists of three steps depicted in Figure 4:

- (1) Irradiation data on CUASO location is determined for each day of the year based on the CRESESB data;
- (2) The irradiance is derived from the amount of energy that can be incident on a PV array over the length of the day;
- (3) The electrical output power in alternating current (AC) is determined as a percentage of the PV capacity in direct current (DC), i.e., the rated DC PV power.

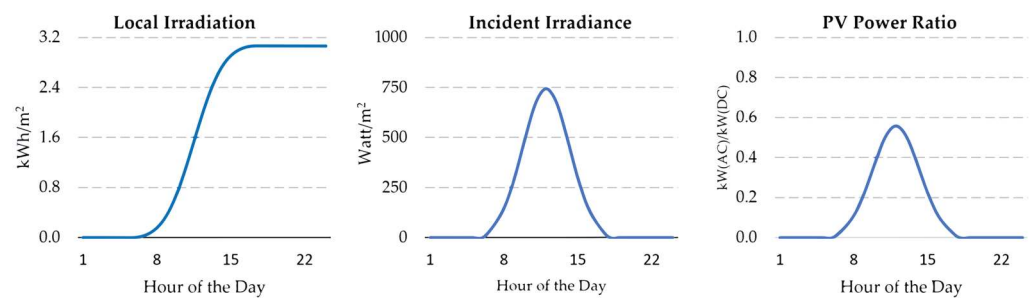


**Figure 4.** Method used to determine the output power generated by a PV system.

Determining step 3 from step 2 required the assumption that the overall PV system performance ratio was 75% and that inverters' power factor was unitary.

The method described above thus produced 365 curves (as in step 3) which gives the ratio of the AC output power over the rated DC PV power. This ratio is of great importance when many power flow runs should be performed with multiple PV system capacities (Section 2.2). With each curve then it is possible to determine the corresponding AC power output along any specific day and hour given any PV system capacity. Hence the synthetic series has 8760 hourly data.

Figure 5 is a set of superposed PV power ratio curves, grouped by month. Hence, values on the vertical axis are dimensionless while the horizontal axis indicates the hours of the day.

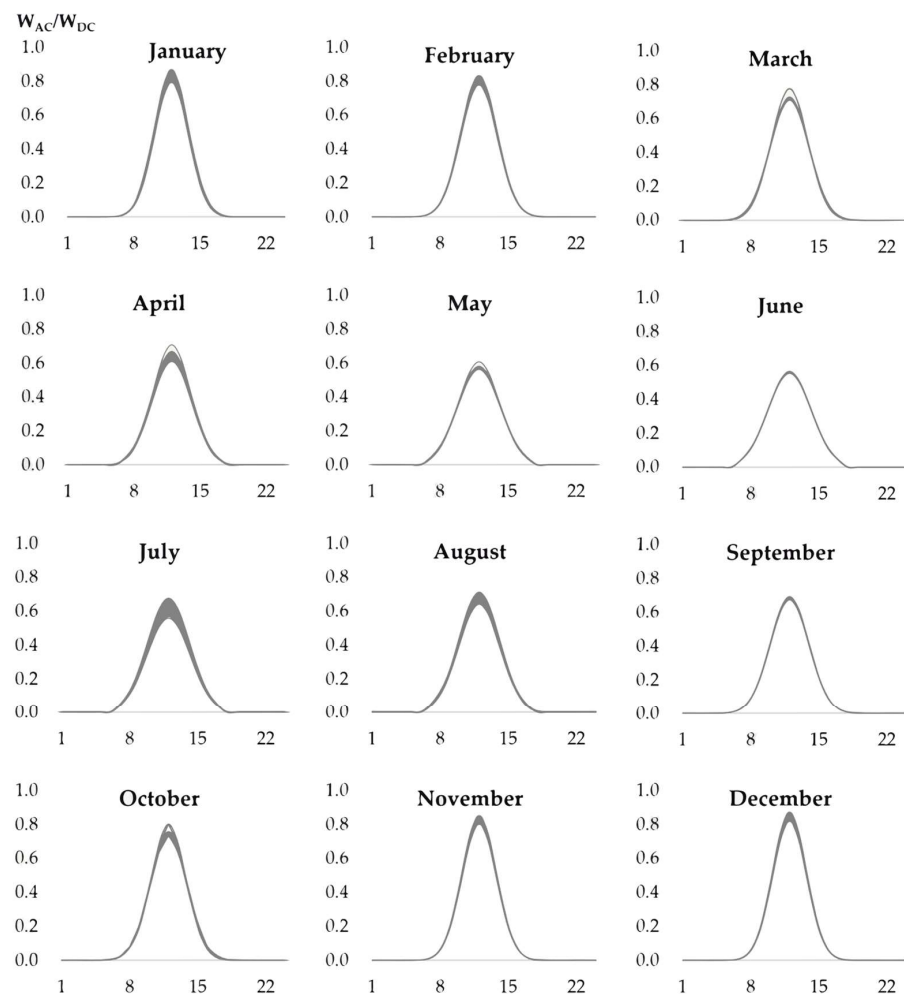


**Figure 5.** Power ratio curves simulated, monthly grouped.

### 3. Materials and Methods

This section presents detailed information used for the implemented methodology.

#### 3.1. An Algorithm for Power Flow Analysis

To determine HC in distribution grids, it is necessary to run steady-state power flow simulations as a tool to check whether voltage or current limits will be violated. An algorithm was implemented based on the method proposed by Teng (2003), which is simpler (compared to traditional methods), robust, and quicker to converge. The method can be applied to radial or weakly meshed circuits, which are most suitable for this case study. The method defines two matrices based on the circuit topology: BIBC matrix (Bus Injection—Branch Current) and BCBV matrix (Branch Current—Bus Voltage) [18].

An advantage of the method is that both matrices remain constant during the iterative calculation. Figure 6 shows a simplified diagram of a 6-bus circuit that will be used to demonstrate how this method works.

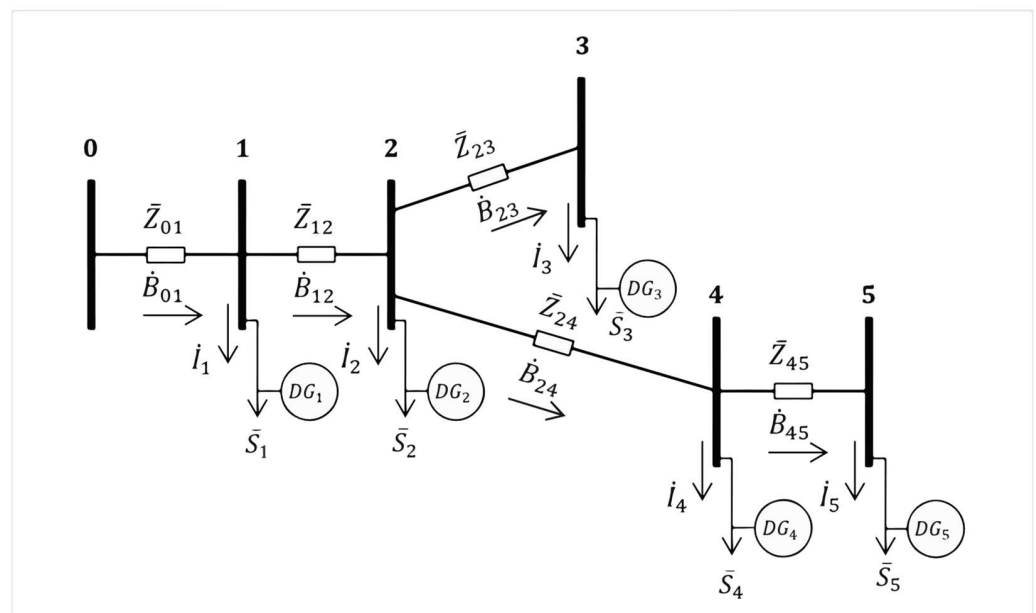


**Figure 6.** Simplified diagram of a 6-bus circuit. Where:  $\dot{U}_i$  is the voltage phasor at bus  $i$ ;  $\dot{I}_i$  is the current phasor at bus  $i$ ;  $\bar{Z}_{i,j}$  is the branch impedance between bus  $i$  and bus  $j$ ;  $\dot{B}_{i,j}$  is the branch current phasor between bus  $i$  and bus  $j$ ;  $DG_i$  is the PV-DG, if any, at bus  $i$ ;  $\bar{S}_i$  is the complex power at bus  $i$ .

Bus 0 is the reference bus that represents the substation which provides the voltage and the angle reference ( $V\theta$  bus). As distributed generators are usually smaller in capacity compared to conventional generators, DG is modeled as a negative load [19]. Thus, any bus with PV-DG can be modeled as a PQ bus [20] in which the values of active and reactive power are known. Therefore, positive values of current indicate that the bus absorbs power and negative values indicate that current is injected into the bus by the corresponding  $DG_i$ .

$$\bar{S}_i = (P_{L i} - P_{GD i}) + j(Q_{L i} - Q_{GD i}), \quad (1)$$

where:

$P_{GD i}$  is the active power generated by PV-DG at bus  $i$ ;

$P_{L i}$  is the power consumed by the load at bus  $i$ ;

$Q_{GD i}$  is the reactive power generated by PV-DG at bus  $i$ ;

$Q_{L i}$  is the reactive power consumed by the load at bus  $i$ ;

Thus,

$$I_i = \left( \frac{\bar{S}_i}{\dot{U}_i} \right)^* = \frac{(P_{Li} - P_{GD i}) - j(Q_{Li} - Q_{GD i})}{\dot{U}_i^*}, \tag{2}$$

$\dot{U}_i^*$  is the voltage complex conjugate at bus  $i$ .

Applying Kirchhoff's current law, the branch currents are:

$$\begin{aligned} \dot{B}_{01} &= \dot{I}_1 + \dot{I}_2 + \dot{I}_3 + \dot{I}_4 + \dot{I}_5 \\ \dot{B}_{12} &= \dot{I}_2 + \dot{I}_3 + \dot{I}_4 + \dot{I}_5 \\ \dot{B}_{23} &= \dot{I}_3 \\ \dot{B}_{24} &= \dot{I}_4 + \dot{I}_5 \\ \dot{B}_{45} &= \dot{I}_5 \end{aligned} \tag{3}$$

The set of equations of the linear system above can be represented in the equation matrix form:

$$\begin{bmatrix} \dot{B}_{01} \\ \dot{B}_{12} \\ \dot{B}_{23} \\ \dot{B}_{24} \\ \dot{B}_{45} \end{bmatrix} = \begin{bmatrix} 1 & 1 & 1 & 1 & 1 \\ 0 & 1 & 1 & 1 & 1 \\ 0 & 0 & 1 & 0 & 0 \\ 0 & 0 & 0 & 1 & 1 \\ 0 & 0 & 0 & 0 & 1 \end{bmatrix} \cdot \begin{bmatrix} \dot{I}_1 \\ \dot{I}_2 \\ \dot{I}_3 \\ \dot{I}_4 \\ \dot{I}_5 \end{bmatrix} \tag{4}$$

The linear system Equation (4) can be summarized as follows:

$$[\dot{B}] = [BIBC] \cdot [\dot{I}] \tag{5}$$

By Ohm's law:

$$\begin{aligned} \dot{U}_5 &= \dot{U}_4 - \bar{Z}_{45} \cdot \dot{B}_{45} \\ \dot{U}_4 &= \dot{U}_2 - \bar{Z}_{24} \cdot \dot{B}_{24} \\ \dot{U}_3 &= \dot{U}_2 - \bar{Z}_{23} \cdot \dot{B}_{23} \\ \dot{U}_2 &= \dot{U}_1 - \bar{Z}_{12} \cdot \dot{B}_{12} \\ \dot{U}_1 &= \dot{U}_0 - \bar{Z}_{01} \cdot \dot{B}_{01} \end{aligned} \tag{6}$$

∴

$$\begin{bmatrix} \dot{U}_0 \\ \dot{U}_0 \\ \dot{U}_0 \\ \dot{U}_0 \\ \dot{U}_0 \end{bmatrix} - \begin{bmatrix} \dot{U}_1 \\ \dot{U}_2 \\ \dot{U}_3 \\ \dot{U}_4 \\ \dot{U}_5 \end{bmatrix} = \begin{bmatrix} \bar{Z}_{01} & 0 & 0 & 0 & 0 \\ \bar{Z}_{01} & \bar{Z}_{12} & 0 & 0 & 0 \\ \bar{Z}_{01} & \bar{Z}_{12} & \bar{Z}_{23} & 0 & 0 \\ \bar{Z}_{01} & \bar{Z}_{12} & 0 & \bar{Z}_{24} & 0 \\ \bar{Z}_{01} & \bar{Z}_{12} & 0 & \bar{Z}_{24} & \bar{Z}_{45} \end{bmatrix} \cdot \begin{bmatrix} \dot{B}_{01} \\ \dot{B}_{12} \\ \dot{B}_{23} \\ \dot{B}_{24} \\ \dot{B}_{45} \end{bmatrix} \tag{7}$$

So, Equation (7) can be summarized as follows:

$$[\Delta \dot{U}] = [BCBV] \cdot [\dot{B}] \tag{8}$$

Replacing Equation (5) in Equation (8):

$$[\Delta \dot{U}] = [BCBV] \cdot [BIBC] \cdot [\dot{I}] \tag{9}$$

The multiplication of the BCBV and BIBC matrices results in the DLF (Distribution Load Flow) matrix of the same dimension that also remains constant throughout the iterative process. DLF matrix relates the voltage delta from bus  $i$  to bus 0 and the current injection at bus  $i$ . In this example:

$$DLF = \begin{bmatrix} \bar{Z}_{01} & \bar{Z}_{01} & \bar{Z}_{01} & \bar{Z}_{01} & \bar{Z}_{01} \\ \bar{Z}_{01} & \bar{Z}_{01} + \bar{Z}_{12} & \bar{Z}_{01} + \bar{Z}_{12} & \bar{Z}_{01} + \bar{Z}_{12} & \bar{Z}_{01} + \bar{Z}_{12} \\ \bar{Z}_{01} & \bar{Z}_{01} + \bar{Z}_{12} & \bar{Z}_{01} + \bar{Z}_{12} + \bar{Z}_{23} & \bar{Z}_{01} + \bar{Z}_{12} & \bar{Z}_{01} + \bar{Z}_{12} \\ \bar{Z}_{01} & \bar{Z}_{01} + \bar{Z}_{12} & \bar{Z}_{01} + \bar{Z}_{12} & \bar{Z}_{01} + \bar{Z}_{12} + \bar{Z}_{24} & \bar{Z}_{01} + \bar{Z}_{12} + \bar{Z}_{24} \\ \bar{Z}_{01} & \bar{Z}_{01} + \bar{Z}_{12} & \bar{Z}_{01} + \bar{Z}_{12} & \bar{Z}_{01} + \bar{Z}_{12} + \bar{Z}_{24} & \bar{Z}_{01} + \bar{Z}_{12} + \bar{Z}_{24} + \bar{Z}_{45} \end{bmatrix} \quad (10)$$

Then Equation (11) shows how the voltage delta at each bus is related to its current injection.

$$[\Delta \dot{U}] = [DLF] \cdot [\dot{i}] \quad (11)$$

All DLF elements are complex numbers. The main diagonal elements are the simple sum of the impedances of the branches from bus 0 to any bus  $i$  considering that there is only one path connecting the reference bus to any other selected bus. Finally, the voltage at each bus can be determined with Equation (12).

$$[\dot{U}] = [\dot{U}_0] - [\Delta \dot{U}] \quad (12)$$

The implemented algorithm calculates iteratively the current injection matrix  $[\dot{i}]$  by Equation (2), the voltage delta matrix  $[\Delta \dot{U}]$  by Equation (11), and bus voltage matrix  $[\dot{U}]$  by Equation (12). The branch current matrix  $[\dot{B}]$  is calculated by Equation (5) after the iterative process has ended. Figure 7 shows a diagram of the algorithm implemented for iterative power flow calculation.

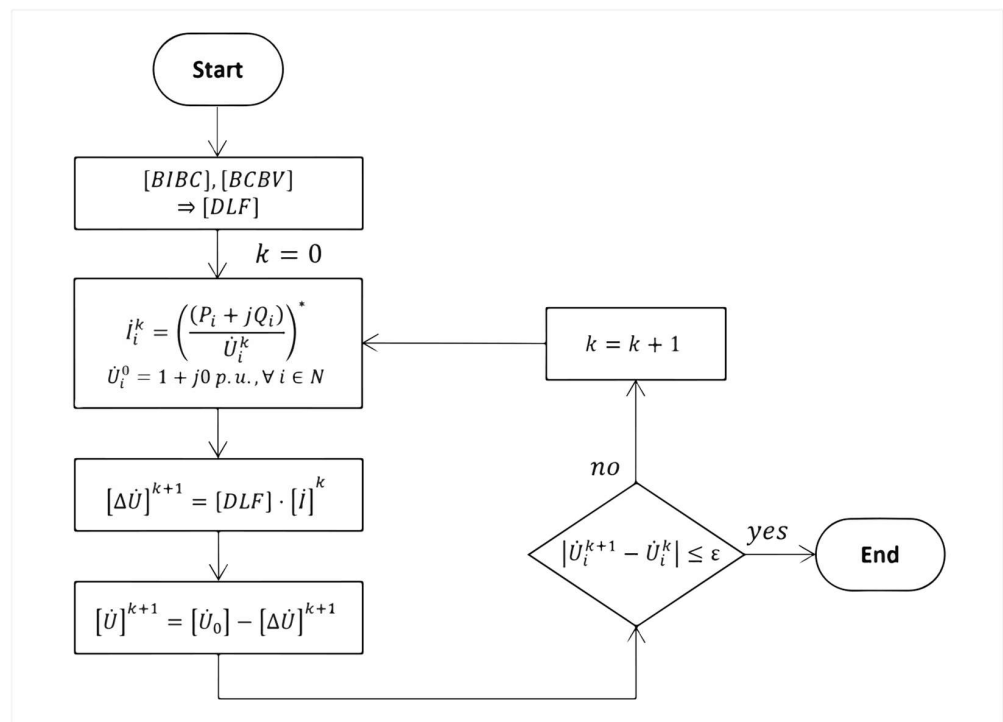


**Figure 7.** Diagram of the algorithm implemented for iterative power flow calculation. The (\*) indicates the complex conjugate of the expression.

The algorithm was coded in VBA within an Excel macro. The DLF matrix was calculated in a spreadsheet with the manual entry of the BIBC and BCBV matrices. At the beginning of the macro execution, the iteration counter was reset ( $k = 0$ ), and the voltage on all buses was equaled to the voltage of the reference bus:  $\dot{U}_i^0 = 1 + j0 p.u.$  As long as the

voltage deviation at the same bus in subsequent iterations was greater than the allowable deviation  $\epsilon$ , the counter was incremented ( $k = k + 1$ ).

### 3.2. Approach Used to Estimate USP-105 Hosting Capacity

Although the match of maximum PV power with minimum load is unlikely, a static and worst-case-based scenario approach was considered using all data presented in the previous sections. However, in this case study, it was not convenient to use the minimum load, which was observed at 3 a.m. (when there is no PV generation), with the maximum PV power possible. Instead, two specific moments were considered: (i) the lowest load at noon (1963.4 kVA) which occurred at hour 3108 of the year and the corresponding PV power in the same hour and day, and similarly, (ii) the highest load value observed at noon (4715.1 kVA) which occurred at hour 1788 and its corresponding PV power. Both moments will be hereinafter referred to as lowest load at noon (LLN) and highest load at noon (HLN), respectively.

The code in VBA automatically increments PV capacity in proportion to the annual active peak power plus the existing PV-DG capacity, if any, at the corresponding bus. The reason for this is to increase the coincidence between the bus load and the PV generation, that is, to maximize the power consumed instantaneously by the bus load which was provided by the PV system interconnected close to it, and consequently minimize power loss and voltage rise. Table 2 shows the active peak power at each bus load read from load data.

**Table 2.** Annual active peak power at each bus load and existing PV-DG.

Location	Bus No.	Active Peak Power (kW)	Existing PV-DG Power (kW)
IEE	2	42.4	234.0 <sup>1</sup>
PUSP-C	4	175.5	
NUCEL	6	144.0	
HU	8	842.7	84.0
ICB III	11	224.8	
FOFITO	12	54.8	
FO	14	511.0	
ICB IV	16	466.9	
FMVZ	17	518.8	
ICB II	19	412.2	
ICB I	20	401.8	
IB	22	593.9	

<sup>1</sup> (156 + 78). See Section 2.2.

The voltage rise limit established for the HC assessment in any bus is 1.0 *p.u.*, although this is not a technically unacceptable limit according to Brazilian standards. The voltage supplied becomes critical if it is less than 90% of the voltage reference (in this case 13.8 kV) or greater than 105%.

The Figure 8 describes the procedure to estimate the HC:

The  $\epsilon$  used to converge the power flow solution was 0.00001.

It is important to point out that the selected ampacity limit is the actual derated current-carrying capacity according to the Brazilian Association of Technical Standards NBR 14039:2005 (IEC based) [21] and the derated current-carrying capacities of each conductor can be seen in the Figure 1.

If any violation is detected, the algorithm is able to read the last PV-DG capacity at each bus before the WHILE loop stops. The sum of all twelve PV capacities is the amount of PV-DG that the USP-105 can accommodate.

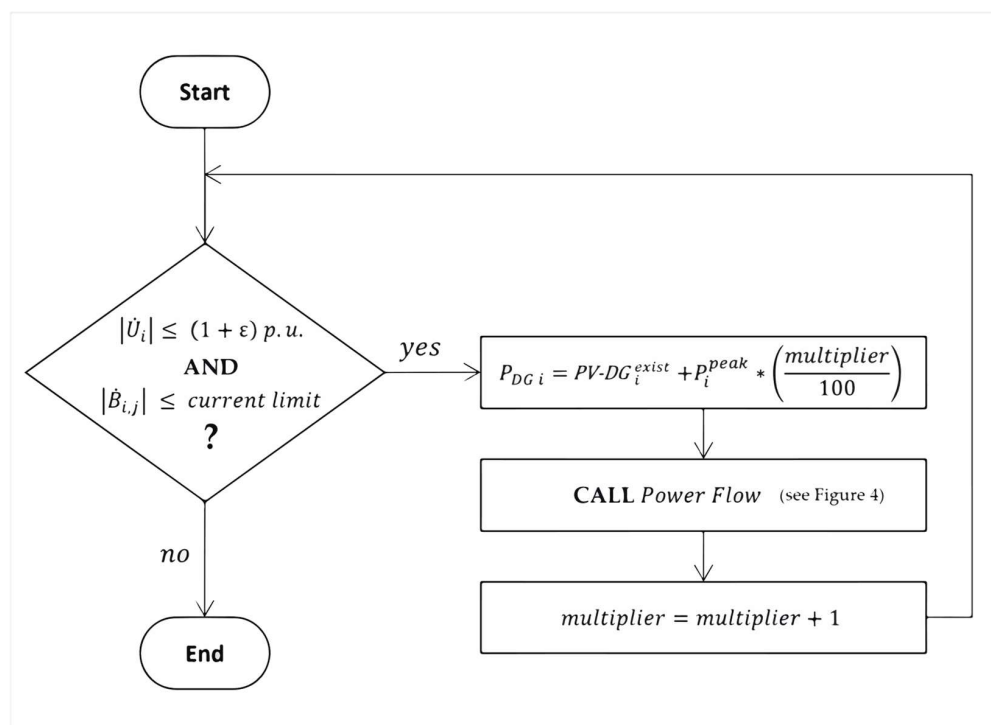


Figure 8. Diagram of the procedure to estimate the hosting capacity.

#### 4. Results

Three simulations were performed. In these simulations, the power flow solution converged in two or three iterations and the simulation runs took from some seconds to a few minutes depending on the initial multiplier chosen.

##### 4.1. HC Estimate for Dispersed PV-DG

The first simulation returned the HC estimate for LLN and HLN. Both moments were considered in a particular scenario in which the PV-DG at USP-105 was deployed with twelve PV systems installed, at once, and as close as possible to the load centers, at buses 2, 4, 6, 8, 11, 12, 14, 16, 17, 19, 20, and 22 (see Figure 1). Table 3 shows solutions for dispersed PV-DG for LLN and HLN.

Table 3. PV-DG capacity at each bus for LLN and HLN.

Location	Bus No.	PV-DG (kW) for LLN	PV-DG (kW) for HLN
IEE	2	278.9	323.8
PUSP-C	4	186.1	372.1
NUCEL	6	152.7	305.3
HU	8	977.8	187.0
ICB III	11	238.2	476.5
FOFITO	12	58.1	116.2
FO	14	541.6	1083.3
ICB IV	16	494.9	989.7
FMVZ	17	550.0	1100.0
ICB II	19	436.9	873.8
ICB I	20	425.9	851.8
IB	22	629.5	1259.0
		4970.6	9622.6

The first HC estimate (4970.6 kW) resulted when the voltage limit was at one increment step to be reached at bus 2 (IEE) and at bus 17 (FMVZ). The second HC estimate (9622.6 kW)

resulted when the voltage limit was at one increment step to be reached at the same buses (2 and 17).

Based on the previous results, two situations were tested with the objective of monitoring voltage and current limits. The first situation considers the deployment of dispersed PV-DG up to the previously determined lower HC estimate (4970.6 kW) for HLN, and the second situation considers the deployment of dispersed PV-DG up to the higher HC estimate (9622.6 kW) for LLN. Both situations were tested with a simple power flow run; in the first test no violation was triggered, and the second test resulted in overvoltage in all buses. Table 4 summarizes both situations tested.

**Table 4.** Tested situations with HC values for dispersed PV-DG.

Tested Situation	PV-DG (kW) <sup>1</sup>	When	Violation
Lower HC with HLN	4970.6	HLN (4715.1 kVA)	No violation
Higher HC with LLN	9622.6	LLN (1963.4 kVA)	Voltage > 1.0 p.u. at all buses

<sup>1</sup> Dispersed PV-DG according to Table 3.

Therefore, the result that should be taken as a USP-105 circuit HC estimate is 4970.6 kW, as shown in Table 3. This value of HC assures that no limit is exceeded for any load varying from the LLN to the HLN. Figures 9 and 10 show the voltage profile throughout the length of the main feeder with and without the deployment of dispersed 4970.6 kW for LLN and HLN, respectively.

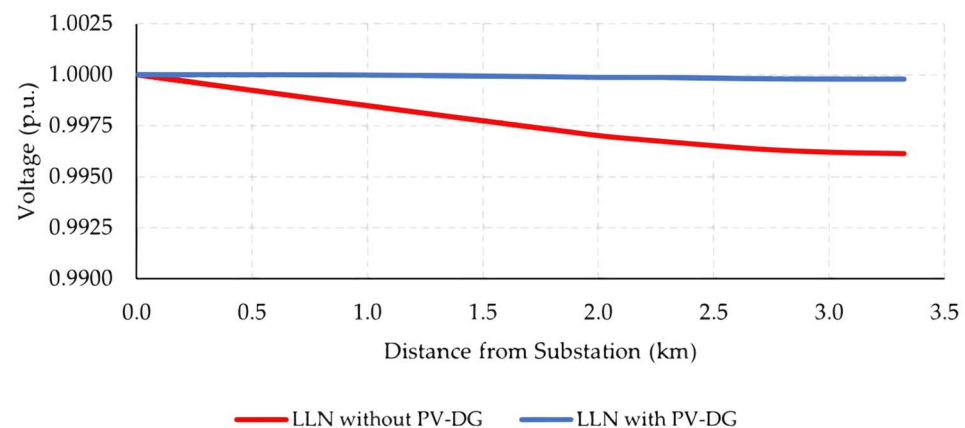


**Figure 9.** Voltage profile with and without dispersed PV-DG deployment for LLN.

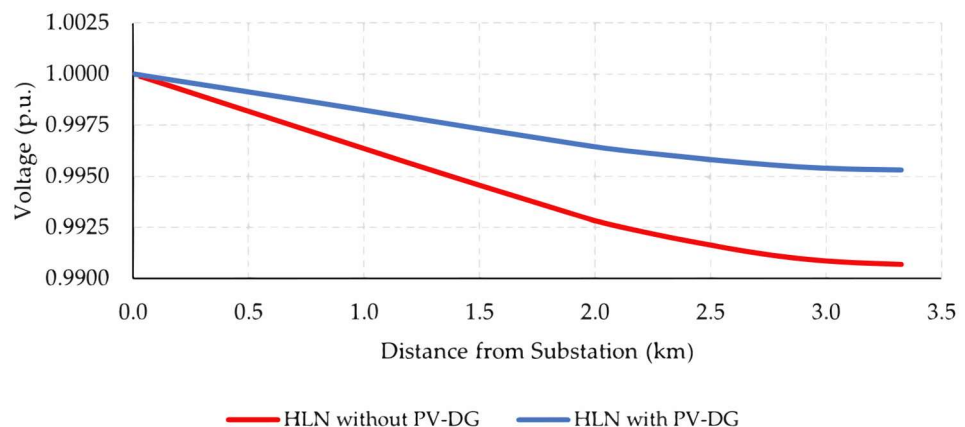


**Figure 10.** Voltage profile with and without dispersed PV-DG deployment for HLN.

For both LLN and HLN, the presence of PV-DG raised the buses' voltage.

#### 4.2. HC Estimate for Concentrated PV-DG

The second simulation returned the HC estimate for concentrated PV-DG in two situations: (i) when PV-DG is installed as close as possible to the substation (ETD-USP) at IEE (bus 2) only, and (ii) when PV-DG is installed at IB (bus 22) only. Tables 5 and 6 show the PV capacity that can be accommodated by the circuit for LLN and HLN, respectively.

**Table 5.** HC estimates for concentrated PV-DG for LLN.

Scenario	Installed at	PV-DG (kW)	Limiting Performance Index
Closest to ETD-USP	IEE (bus 2)	4166.5	Voltage
Furthest to ETD-USP	IB (bus 22)	3230.7	Voltage

**Table 6.** HC estimates for concentrated PV-DG for HLN.

Scenario	Installed at	PV-DG (kW)	Limiting Performance Index
Closest to ETD-USP	IEE (bus 2)	3620.9	Current
Furthest to ETD-USP	IB (bus 22)	4326.3	Current

The results for concentrated PV-DG reveal that the HC estimates depend directly on the bus load where the PV system is interconnected. Other HC estimates would provide different results if simulations were run independently at any other buses, if the USP-105 is at its lowest or highest load. For the sake of this case study, one should simulate the concentrated PV capacity in each of the 12 units in every hour of the year to compare the results.

#### 4.3. Concentrated versus Dispersed PV-DG Deployment

The third and last simulation was a simple power flow run that returned all buses' voltages for LLN and HLN in four different cases while considering the previously determined HC estimate: (i) no PV-DG deployment (base case), (ii) PV-DG is concentrated closest to ETD-USP at IEE (bus 2), (iii) PV-DG is dispersed as shown in Table 3, and (iv) PV-DG is concentrated furthest to ETD-USP at IB (bus 22). This simulation considered the following capacities: (a) 4970.6 kW for dispersed PV-DG, (b) 3620.9 kW for the PV-DG deployed closest to the substation, and (c) 3230.7 kW for the PV-DG deployed furthest to the substation. Figures 11 and 12 show the voltage profile along the main feeder of the USP-105 for LLN and HLN, respectively.

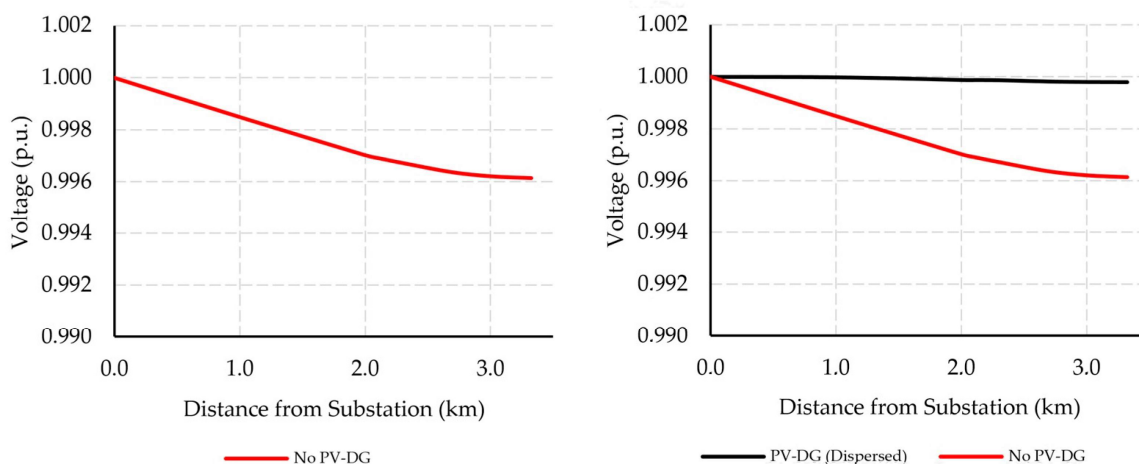


**Figure 11.** Cont.

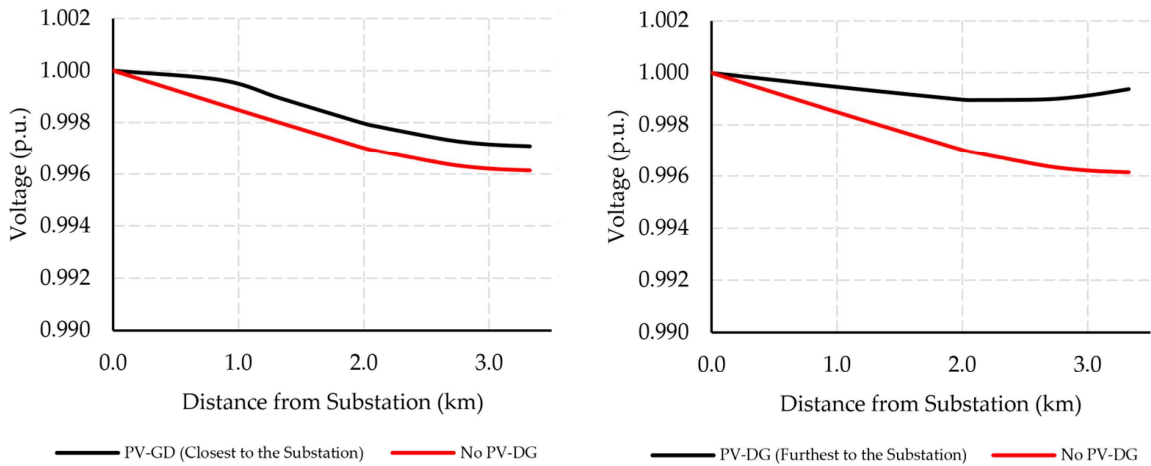


Figure 11. USP-105 main feeder voltage profile simulated for LLN.

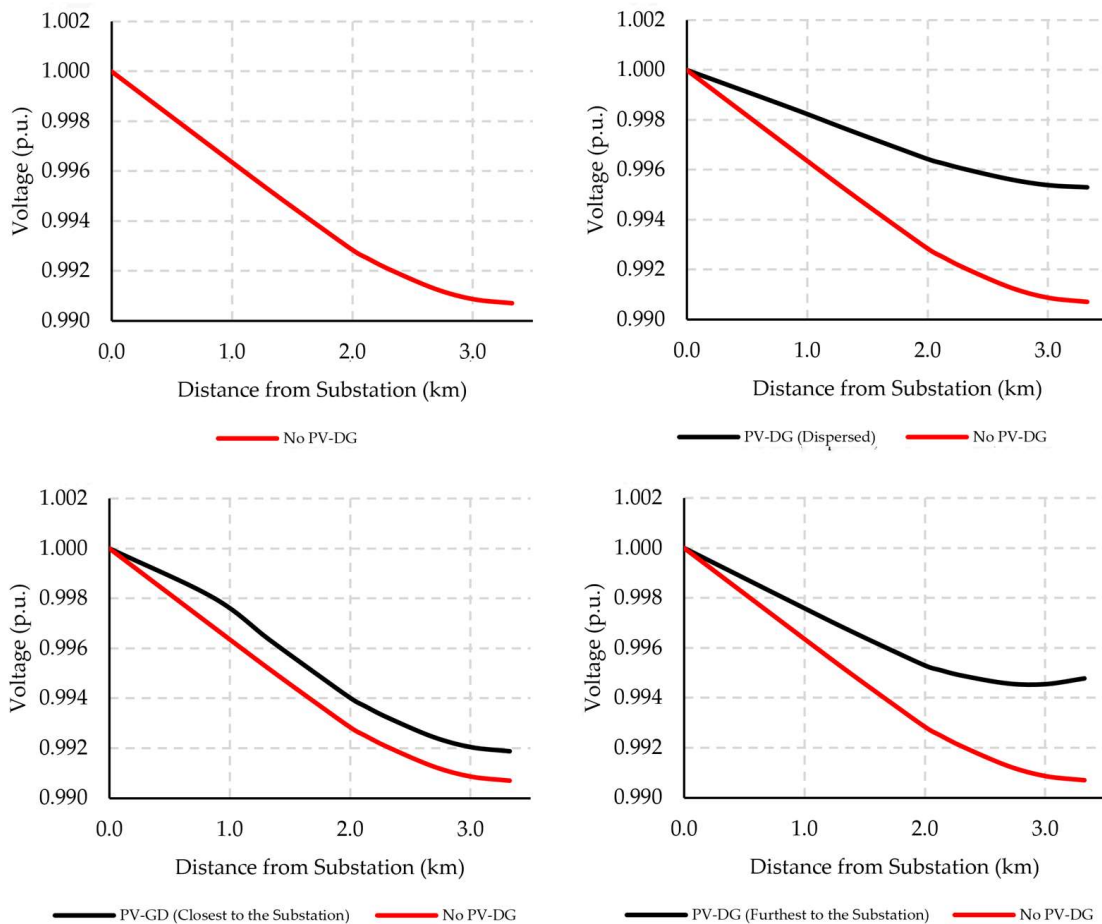


Figure 12. USP-105 main feeder voltage profile simulated for HLN.

5. Discussion

This paper shows that it is possible to assess HC value considering performance indices and their limits as well as a deterministic approach. The first simulation shows, as expected, that HC is directly proportional to load, since the higher the load to which the PV-DG is interconnected, the higher the PV power that is instantly consumed. The second simulation shows that HC is higher when PV-DG is concentrated closest to the substation compared to PV-DG concentrated furthest to the substation, as observed by

Horowitz et al. (2018) and McAllister et al. (2019). Nonetheless, dispersed PV-DG not only increased the HC estimate to 4970.6 kW but also improved the voltage profile along the USP-105 main feeder. This HC value corresponds to 103% of the circuit's peak load (see Table 3), which is substantially more significant than the 15% rule of thumb mentioned before that. In this case, the study would return a mere 721 kW as the maximum PV-DG capacity that USP-105 could host. Although this rule of thumb is conservative, it is ambiguous since it does not specify whether the maximum capacity should be concentrated or dispersed. As shown in Table 3 for LLN, none except for HU (bus 8) would admit this 721 kW at once.

The deployment of dispersed 4970.6 kW reduced the peak load by 9% to 4363.5 kVA; it could not be less because of two main reasons: (i) the USP-105 load has a low power factor of around 0.8 most of the year, and PV-DG is providing active power only, and (ii) load daily high and PV peak generation are usually from 2 to 5 h apart.

Nevertheless, the USP-105 circuit HC estimate is not the ultimate result. A different dispersion of the same PV-DG capacity would result in a different estimate; the same would happen if a stochastic method were used. The HC estimate would differ significantly if more performance indices, such as protection issues, were selected and uncertainties were considered. On the other hand, the HC estimate is likely to be underestimated because a static and worst-case-based scenario approach was chosen. The advantage of using a static and worst-case-based scenario approach is that it is easier to implement. Furthermore, PV-DG deployment would help to reduce the circuit's loading, increasing the conductor's life span and reducing the power losses.

It is important to point out that PV-DG improves the voltage profile throughout the main feeder compared to when no PV-DG is deployed, especially when the PV-DG is dispersed (Figures 9 and 10), keeping the voltage along the main feeder slightly below 1.0 p.u. When the PV-DG is concentrated, the voltage tends to rise more rapidly; another issue for the concentrated PV-DG is that the current limit will be reached earlier due to the laterals' ampacity. Finally, Figures 11 and 12 show that the voltage profile is better improved when PV-DG is dispersed rather than concentrated closest or furthest to the substation. In any situation, the voltage profile was improved compared to no PV-DG deployment at all. However, as discussed before, the capacity of concentrated PV-DG is significantly lower than when the PV-DG deployment is dispersed (see Tables 5 and 6).

Figures 11 and 12 also indicate that the PV-DG closest to the substation did not alter the voltage curve but shifted it up, providing complementary power to the substation's supply.

## 6. Conclusions

Estimating HC using deterministic methods is subject to considerable uncertainty, as unlikely scenarios may not reflect a particular reality accurately. However, such methods provide an overview of a circuit or feeder's ability to accommodate PV power, including how it behaves based on the location and capacity of the PV-DG deployed.

The HC assessment helps utilities to screen interconnection requests and to set limits for PV capacity on specific feeders so that PV-DG capacity will not grow unrestrictedly, nor will it be lower than it could if any rule of thumb were applied instead.

In this case study of the underground feeder, USP-105, the HC assessment was performed based on a steady-state and worst-case-based scenario used to run deterministic power flow simulations. The results revealed that PV-DG is better dispersed rather than concentrated. When concentrated, the HC is proportional to load and to ensure that the PV capacity will always fit, USP-105 can accommodate 103% of its peak load or 4970.6 kW, which reduced by 9% the circuit's annual peak load. This value is far beyond the 15% limit (or 721 kW) imposed by rules of thumb.

The PV-DG deployed closest to the substation can be seen as a substation-like source providing complementary power and energy to all loads downstream. The final voltage profile resembles the voltage profile with no PV-DG. The PV-DG deployed furthest to the

substation has lower HC, while the dispersed PV-DG shows a better voltage profile and a higher HC value.

The results demonstrate that installing PV systems closer to the loads is better than interconnecting a single system of greater capacity. Besides, the direct and simplified approach selected to estimate HC values may help utilities to benefit from estimating specific circuits' HC quickly in an effortless manner and substituting generalist and conservative rules of thumb with a more accurate method. Finally, utilities can actively indicate the optimum location for PV deployment and benefit from it if a circuit is congested or reporting voltage sags at specific locations.

**Author Contributions:** Conceptualization, methodology, formal analysis, writing—original draft preparation, I.C.; resources, writing—review and editing, W.B.; supervision, I.L.S. All authors have read and agreed to the published version of the manuscript.

**Funding:** The authors acknowledge the financial support from the Institute of Energy and Environment of University of São Paulo (IEE-USP), Center for Analysis, Planning and Energy Resources Development (CPLN), FUSP project number 3827: “From organic waste to bioenergy and biofertilizers: a proposal for innovation in management, regulation and technologies and integration of industrial production chains” as well as from Enel Distribuição São Paulo in partnership with the Brazilian Electricity Regulatory Agency (ANEEL), Priority Energy and Strategic R&D project: “Energy Efficiency and Minigeneration in Public University Institutions”, grant number 00390-1086/2018.

**Conflicts of Interest:** The authors declare no conflict of interest.

## Nomenclature

BCBV	“Branch Current—Bus Voltage” matrix
BIBC	“Bus Injection—Branch Current” matrix
CUASO	Cidade Universitária “Armando de Salles Oliveira” (campus of the University of São Paulo)
DG	distributed generation
DLF	“Distribution Load Flow” matrix
ETD-USP	campus substation
HC	hosting capacity
HLN	highest load at noon
IB	Institute of Biosciences
IEE	Institute of Energy and Environment
LLN	lowest load at noon
PV	photovoltaic
PV-DG	photovoltaic distributed generation
USP-105	circuit “105” of the campus

## References

- IRENA. Global Trends. 2022. Available online: <https://irena.org/Statistics/View-Data-by-Topic/Costs/Global-Trends> (accessed on 28 January 2023).
- IRENA. Solar Energy. 2022. Available online: <https://www.irena.org/Energy-Transition/Technology/Solar-energy> (accessed on 28 January 2023).
- ANEEL. Distributed Generation. 2022. Available online: <https://app.powerbi.com/view?r=eyJrIjoiZjM4NjM0OWYtN2IwZS00YjViLTllMjItN2E5MzBkN2ZlMzVklwiidCI6IjQwZDZmOWI4LWVjYyTctNDZhMi05MmQ0LWVhNGU5YzAxNzBIMSIsImMiOiR9> (accessed on 21 March 2023).
- Gaunt, C.T.; Namanya, E.; Herman, R. Voltage Modelling of LV Feeders with Dispersed Generation: Limits of penetration of randomly connected photovoltaic generation. *Electr. Power Syst. Res.* **2017**, *143*, 1–6. [[CrossRef](#)]
- Gil, H.A.; Joos, G. On the Quantification of the Network Capacity Deferral Value of Distributed Generation. *IEEE Trans. Power Syst.* **2006**, *21*, 1592–1599. [[CrossRef](#)]
- Widén, J.; Wäckelgård, E.; Paatero, J.; Lund, P. Impacts of Distributed Photovoltaics on Network Voltages: Stochastic simulations of three Swedish low-voltage distribution grids. *Electr. Power Syst. Res.* **2010**, *80*, 1562–1571. [[CrossRef](#)]
- Seguin, R.; Woyak, J.; Costyk, D.; Hambrick, J.; Mather, B. *High-Penetration PV Integration Handbook for Distribution Engineers*; Technical Report NREL/TP-5D00-63114; National Renewable Energy Laboratory (NREL): Golden, CO, USA, 2016.

8. Hoke, A.; Butler, R.; Hambrick, J.; Kroposki, B. Steady-State Analysis of Maximum Photovoltaic Penetration Levels on Typical Distribution Feeders. *IEEE Trans. Sustain. Energy* **2013**, *4*, 350–357. [[CrossRef](#)]
9. Ismael, S.M.; Aleem, S.H.A.; Abdelaziz, A.Y.; Zobia, A.F. State-of-the-Art of Hosting Capacity in Modern Power Systems with Distributed Generation. *Renew. Energy* **2019**, *130*, 1002–1020. [[CrossRef](#)]
10. Mulenga, E.; Bollen, M.H.J.; Etherden, N. A review of Hosting Capacity Quantification Methods for Photovoltaics in Low-voltage Distribution Grids. *Electr. Power Energy Syst.* **2020**, *115*, 105445. [[CrossRef](#)]
11. Bollen, M.H.J.; Rönnberg, S.K. Hosting Capacity of the Power Grid for Renewable Electricity Production and New Large Consumption Equipment. *Energies* **2017**, *10*, 1325. [[CrossRef](#)]
12. Baldenko, N.; Behzadirafi, S. Determination of Photovoltaic Hosting Capacity on Radial Electric Distribution Feeders. In Proceedings of the 2016 IEEE International Conference on Power System Technology (POWERCON), Wollongong, NSW, Australia, 28 September–1 October 2016.
13. McAllister, R.; Manning, D.; Bird, L.; Coddington, M.H.; Volpi, C.M. *New Approaches to Distributed PV Interconnection: Implementation Considerations for Addressing Emerging Issues*; NREL: Golden, CO, USA, 2019; Technical Report NREL/TP-6A20-72038.
14. Etherden, N. Increasing the Hosting Capacity of Distributed Energy Resources Using Storage and Communication. Ph.D. Thesis, Luleå University of Technology, Lulea, Sweden, 2014.
15. Shayani, R.A.; Oliveira, M.A.G. Photovoltaic Generation Penetration Limits in Radial Distribution Systems. *IEEE Trans. Power Syst.* **2011**, *26*, 1625–1631. [[CrossRef](#)]
16. Horowitz, K.A.; Ding, F.; Mather, B.A.; Palmintier, B.S. *The Cost of Distribution System Upgrades to Accommodate Increasing Penetrations of Distributed Photovoltaic Systems on Real Feeders in the United States*; NREL: Golden, CO, USA, 2018; Technical Report NREL/TP-6A20-70710.
17. CRESESB/CEPEL. Solar Potential—SunData. Available online: <http://www.cresesb.cepel.br/index.php?section=sundata&lang=en> (accessed on 28 January 2023).
18. Teng, J. A Direct Approach for Distribution System Load Flow Solutions. *IEEE Trans. Power Deliv.* **2003**, *18*, 882–887. [[CrossRef](#)]
19. Mishra, S.; Das, D.; Paul, S. A Simple Algorithm for Distribution System Load Flow with Distributed Generation. In Proceedings of the International Conference on Recent Advances and Innovations in Engineering (ICRAIE-2014), Jaipur, India, 9–11 May 2014.
20. Parihar, S.S.; Malik, N. Load Flow Analysis of Radial Distribution System with DG and Composite Load Model. In Proceedings of the 2018 International Conference on Power Energy, Environment and Intelligent Control (PEEIC), Greater Noida, India, 13–14 April 2018.
21. *NBR 14039:2005; Instalações elétricas de média tensão (Electrical Installations—Medium Voltage)*. Brazilian Association of Technical Standards: Rio de Janeiro, Brazil, 2005.

**Disclaimer/Publisher’s Note:** The statements, opinions and data contained in all publications are solely those of the individual author(s) and contributor(s) and not of MDPI and/or the editor(s). MDPI and/or the editor(s) disclaim responsibility for any injury to people or property resulting from any ideas, methods, instructions or products referred to in the content.